

## Accepted Manuscript

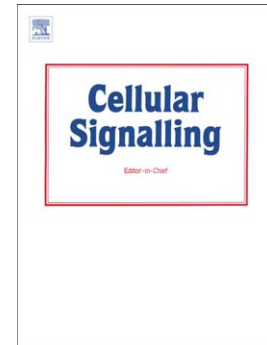
Features of the reversible sensitivity-resistance transition in PI3K/PTEN/AKT signalling network after HER2 inhibition

Alexey Goltsov, Dana Faratian, Simon P. Langdon, Peter Mullen, David J. Harrison, James Bown

PII: S0898-6568(11)00311-1  
DOI: doi: [10.1016/j.cellsig.2011.09.030](https://doi.org/10.1016/j.cellsig.2011.09.030)  
Reference: CLS 7446

To appear in: *Cellular Signalling*

Received date: 9 May 2011  
Revised date: 15 September 2011  
Accepted date: 27 September 2011



Please cite this article as: Alexey Goltsov, Dana Faratian, Simon P. Langdon, Peter Mullen, David J. Harrison, James Bown, Features of the reversible sensitivity-resistance transition in PI3K/PTEN/AKT signalling network after HER2 inhibition, *Cellular Signalling* (2011), doi: [10.1016/j.cellsig.2011.09.030](https://doi.org/10.1016/j.cellsig.2011.09.030)

This is a PDF file of an unedited manuscript that has been accepted for publication. As a service to our customers we are providing this early version of the manuscript. The manuscript will undergo copyediting, typesetting, and review of the resulting proof before it is published in its final form. Please note that during the production process errors may be discovered which could affect the content, and all legal disclaimers that apply to the journal pertain.

## Features of the reversible sensitivity-resistance transition in PI3K/PTEN/AKT signalling network after HER2 inhibition

Alexey Goltsov<sup>a,\*</sup>, Dana Faratian<sup>b</sup>, Simon P Langdon<sup>b</sup>, Peter Mullen<sup>b</sup>, David J Harrison<sup>b</sup>, James Bown<sup>a</sup>

<sup>a</sup> Centre for Research in Informatics and Systems Pathology (CRISP), University of Abertay Dundee, Dundee, DD1 1HG, United Kingdom

<sup>b</sup> Edinburgh Breakthrough Research Unit and Division of Pathology, Western General Hospital, University of Edinburgh, Edinburgh, EH4 2XU, United Kingdom

\* Corresponding author: Alexey Goltsov

Address: CRISP, University of Abertay Dundee, Dundee, DD1 1HG, UK

Tel: +441382 308432

E-mail: a.goltsov@abertay.ac.uk

*Keywords:* RTK inhibitor; pertuzumab; PI3K/PTEN/AKT signalling network; anticancer drug resistance; sensitivity analysis, drug combination.

## Abstract

Systems biology approaches that combine experimental data and theoretical modelling to understand cellular signalling network dynamics offer a useful platform to investigate the mechanisms of resistance to drug interventions and to identify combination drug treatments. Extending our work on modelling the PI3K/PTEN/AKT signalling network (SN), we analyze the sensitivity of the SN output signal, phospho-AKT, to inhibition of HER2 receptor. We model typical aberrations in this SN identified in cancer development and drug resistance: loss of PTEN activity, PI3K and AKT mutations, HER2 overexpression, and overproduction of GSK3 $\beta$  and CK2 kinases controlling PTEN phosphorylation. We show that HER2 inhibition by the monoclonal antibody pertuzumab increases SN sensitivity, both to external signals and to changes in kinetic parameters of the proteins and their expression levels induced by mutations in the SN. This increase in sensitivity arises from the transition of SN functioning from saturation to non-saturation mode in response to HER2 inhibition. PTEN loss or *PI3CA* mutation causes resistance to anti-HER2 inhibitor and leads to the restoration of saturation mode in SN functioning with a consequent decrease in SN sensitivity. We suggest that a drug-induced increase in SN sensitivity to internal perturbations, and specifically mutations, causes SN fragility. In particular, the SN is vulnerable to mutations that compensate for drug action and this may result in a sensitivity-to-resistance transition. The combination of HER2 and PI3K inhibition does not sensitize the SN to internal perturbations (mutations) in the PI3K/PTEN/AKT pathway: this combination treatment provides both synergetic inhibition and may prevent the SN from acquired mutations causing drug resistance. Through combination inhibition treatments, we studied the impact of upstream and downstream interventions to suppress resistance to the HER2 inhibitor in the SN with PTEN loss. Comparison of experimental results of PI3K inhibition in the PTEN upstream pathway with PDK1 inhibition in the PTEN downstream pathway show that upstream inhibition abrogates resistance to pertuzumab more effectively than downstream inhibition. This difference in inhibition effect arises from the compensatory mechanism of an activation loop induced in the downstream pathway by PTEN loss. We highlight that drug target identification for combination anti-cancer therapy needs to account for the mutation effects on the upstream and downstream pathways.

## Introduction

A systems biology approach to the study of anti-cancer drug action on cellular signalling networks (SNs) provides a useful strategy to explore SN output response to input stimuli [1-4], the influence of SN status on drug efficacy [2,5-7], SN target identification for drug design [2,8,9] and development of novel combination therapies [10,11]. An integrative analysis of -omics data revealed that drug efficacy depends on SN sensitivity, which is variable and depends on *de novo* or acquired mutations of receptors/proteins and their expression level [10,12]. The transition of SN response from sensitivity to resistance to drugs results from not only mutations of drug targets but mutations and cross-talk in downstream pathways: For example, mutations in downstream pathways lead to resistance in the case of anti-cancer drugs targeting the ErbB epidermal growth factor receptor (EGFR) family [12-15].

Trastuzumab and pertuzumab, humanised monoclonal antibodies, target extracellular domains of ErbB2/HER2 receptor tyrosine kinase (RTK) and respectively prevent homo- and heterodimerization of the receptors HER2/HER2 and HER2/HER3 which are reported to be the most mitogenic signalling complexes in ovarian and breast cancer [13,16]. RTK inhibitors are an effective therapy against abnormal activation of ErbB signalling and constitutive activation of MAP kinase and PI3K/PTEN/AKT pathways that cause uncontrolled cellular growth [17]. While trastuzumab trials showed a high therapeutic response in tumors with HER2 amplification, pertuzumab (in a phase II trial) targets ovarian and breast cancer with any level of HER2 expression [18,19].

Despite the observed anti-cancer effect of these drugs, the overall analysis of *in vitro* experiments and clinical trials revealed the limitation of these drugs as mono-therapy, less than 35% of HER2<sup>+</sup> patients respond to trastuzumab-based mono-therapy [20]. The results of an extended genetic study showed that aberrant receptor expression together with somatic activation mutations in downstream pathways may be mutually correlated, and generate the tumour phenotype resistant to anti-HER2 therapy [21].

One of the downstream pathways activated by ErbB receptors is the PI3K/PTEN/AKT pathway, which controls AKT activation and plays a key role in cell proliferation, differentiation and survival (see Fig. 1) [12]. Activation of AKT occurs in the PI3K/PTEN/AKT module, which forms a regulatory hub in cellular signalling [13]. This hub includes phosphoinositide 3-kinase (PI3K) and phosphatase PTEN, which control jointly the pool of the second lipid messenger, phosphatidylinositol-3,4,5-trisphosphate (PIP3). PIP3, the

product of PI3K, induces membrane localisation of PH domain-containing proteins, AKT and PDK1. PIP3 binding with AKT enables AKT activation through its phosphorylation by PDK1. PTEN relocates from the cytosol to the membrane and negatively regulates PIP3 pool by its dephosphorylation [22].

Correct regulation of the PIP3 pool in the PI3K/PTEN/AKT module is essential for the fine tuning of signal transduction in the downstream pathway of AKT activation. An integrative genomic and proteomic analysis of breast and other cancers revealed that this regulation hub is vulnerable to mutation, and is observed to be a target of cancer-driving mutations that cause a transition from normal signal transduction to aberrant activation of AKT [23]. This transition blocks the action of the regulator hub, and fine tuned control is lost.

Disruptions to this PI3K/PTEN/AKT pathway are known to lead to drug resistance. Loss of activity of the tumour suppressor PTEN was reported to be determined in nearly 50% of all breast cancers and many other cancers [24,25]. PTEN loss mainly results from PTEN mutations, loss of heterozygosity at the *PTEN* locus, and epigenetic down-regulation of PTEN [26]. Analysis of HER2 positive breast tumours revealed that a PTEN deficit correlates with resistance to trastuzumab-based therapy [27]. Oncogenic mutation of PI3K in the catalytic subunit p110 $\alpha$  encoding *PIK3CA* gene was observed in up to 50% of breast cancers [28] and also conferred resistance to trastuzumab [25]. AKT mutations in the PH domain of AKT1 isoform were identified in 8% of breast cancers, and this mutation causes PIP3-independent activation of AKT1 by recruiting it to the membrane [25].

Joint PTEN loss and *PIK3CA* mutation were reported to be frequently concordant in breast cancer [24,25,28,29]. Analysis of either PTEN status or *PIK3CA* mutation alone limits prognostic assessment for trastuzumab treatment, and that analysis of PTEN and PI3K status in combination is a superior biomarker of the resistance to anti-HER2 therapy [24]. As both mutations activate AKT, this finding suggests redundancy in mutation, the need for two alterations in the single module to activate AKT, or that PTEN loss and PIK3CA mutation contribute differently to carcinogenesis [25].

Mutual correlation of HER2 overexpression and either *PIK3CA* mutation or PTEN loss was found in approximately 25% of HER2<sup>+</sup> breast cancer cases, and are major factor in anti-HER2 therapy [27,30]. It is likely that HER2 overexpression and *PIK3CA* mutation or PTEN loss work together to enhance the activation of AKT. A combination of trastuzumab with PI3K inhibitor (LY294002, wortmannin) was observed to restore the inhibition effect of trastuzumab in HER2<sup>+</sup>, PTEN<sup>-</sup> cell lines [29]. It was proposed to measure the combined status

of HER2, *PIK3CA* and PTEN as a biomarker to predict resistance to anti-HER2 therapy [25,29,31].

These experimental and clinical data support the role of the PI3K/PTEN/AKT pathway as a regulatory hub in the control of cell survival, which undergoes oncogenic mutations causing cancer development and resistance to anti-HER2 therapy. Here, we extend our study of the role of PI3K/PTEN/AKT signalling hub in resistance mechanisms to RTK inhibition in ovarian cancer cells [32,33]. In [32] we elucidated the key role of the tumour suppressor PTEN in resistance to anti-HER2 drugs by analysing the response kinetics of AKT activation to pertuzumab and justified this by the results of survival curve analysis for patients treated with trastuzumab for low and high PTEN expression level.

In [33] we further developed the combined experimental and theoretical approach to study the mechanism underlying resistance to RTK inhibition resulting from aberrant expression of PI3K, PTEN and AKT enzymes. We studied the dose dependence of AKT activation on pertuzumab for different perturbations of the PI3K/PTEN/AKT signalling pathway through manipulation of PI3K and PTEN activities by their inhibition. We introduced control parameter  $\gamma = \text{PTEN}/(\text{PI3K} \cdot \text{AKT})$  which determines the balance of enzyme activities in this cycle. We showed that  $\gamma$  correlates with pertuzumab efficacy for 13 ovarian cancer cell lines with different expression levels of the enzymes involve in this cycle. Together with measurement of the ratio of HER2/HER3 expression levels, parameter  $\gamma$  was shown to be a biomarker of responsiveness of cancer cells to anti-HER2 therapy [33].

In this paper we further explore the PI3K/PTEN/AKT signalling pathway by studying the sensitivity of the SN, i.e., how the output signal of the SN responds to the changes in external stimulus (activation signal and drug intervention) and internal properties of the SN such as catalytic characteristics of the enzymes and their expression levels, which may represent mutations.

We separate out two subsystems of the whole SN: the receptor signalling system (RSS) and the signalling transduction system (STS) and study separately their signal response and sensitivity properties. The RSS subsystem comprises the reaction of ligand with receptor, receptor dimerization and mutual phosphorylation of receptors by receptor tyrosine kinase reactions, with RSS output being phosphorylated receptors (see Fig.1). The STS subsystem has RSS output as the input signal, and comprises PI3K/PTEN/AKT and RAF/MEK/ERK signalling pathways, and STS output signals are phosphorylated ERK and AKT (here, we focus on AKT output only). This method permits us to compare the signal response properties

for ovarian cancer cells (using the PE04 cell line) with similar properties obtained for other cells [1,2,34], by comparing variation over different cell lines in both receptor signaling and signal transduction systems. We derive the relationship between sensitivities of these subsystems and calculate their contribution to the sensitivity of the whole SN.

We analyse the sensitivity of the AKT output signal to HER2 inhibition using computational model of PI3K/PTEN/AKT signaling and modeling activation mutations identified in cancer development and drug resistance. Specifically we consider: loss of PTEN activity, PI3K, AKT mutations, HER2, AKT overexpression, and overproduction of GSK3 $\beta$  and CK2 kinases controlling PTEN phosphorylation. We use sensitivity analysis to elucidate the mechanisms of SN sensitivity change as a result of the sensitivity-to-resistance transition arising from activation mutations and drug action.

Through *in silico* and *in vitro* experiments, we also study combination inhibition of the SN to determine: 1) How to prevent acquired mutations arising from drug intervention and escape from oncogene addiction; and 2) How to restore sensitivity to RTK inhibitors by drug combination at activation mutations in the SN [12]. We consider these problems through the example of PTEN loss leading to pertuzumab resistance and assess *in silico* and *in vitro* the efficacy of the inhibition of drug targets in PTEN upstream and downstream pathways.

## 2. Materials and methods

### 2.1. Computational methods

#### 2.1.1. Kinetic model of RAF/MEK/ERK and PI3K/PTEN/AKT signalling

To study the sensitivity-to-resistance transition and analyse the sensitivity properties of the signalling network to RTK inhibitors we used the kinetic model of RAF/MEK/ERK and PI3K/PTEN/AKT signalling developed in [32]. This model describes the response kinetics of the SN to heregulin (HRG)-induced HER3/HER2 receptor heterodimerisation and the effect of RTK inhibitor, pertuzumab (2C4 antibody), on ERK and AKT activation in the human ovarian carcinoma cell line PE04 [32]. The scheme of the signalling network that corresponds to the model is shown in Fig. 1. In the model we neglected HER4 heterodimerization because HER4 receptor expression was barely detectable in the PE04 cell line [32]. It was found that HER2/HER3 heterodimerization activates the most mitogenic signal and induces cellular growth in PE04 cell line [32] as well as in many other cancer cells *in vitro* [18]. The model

[32] considers only cytosol activation of AKT and ERK, without consideration of nuclear localisation of AKT, ERK, and PTEN [35].

The model was parameterised by experimental data on the phosphorylation kinetics of HER2, ERK, AKT, and PTEN in the absence and presence of pertuzumab and was validated based on experimental data on the different combination effects of PTEN, PI3K, and HER2 inhibition on AKT activation [32,33].

Central to this analysis was the introduction of a control parameter,  $\gamma$ , of the PI3K/PTEN/AKT cycle [33]:

$$\gamma = \frac{v_{PTEN}}{v_{PI3K} \cdot v_{AKT}}, \quad (1)$$

that determined the balance of activities,  $v$ , of PTEN, PI3K, and AKT enzymes

$$v_{PTEN} = \frac{k_{cat,PTEN} PTEN_o}{K_{m,PTEN}}; \quad v_{PI3K} = \frac{k_{cat,PI3K} PI3K_o}{K_{m,PI3K}}; \quad v_{AKT} = \frac{K_{d,AKT}}{AKT_o}.$$

Here  $K_m$  and  $k_{cat}$  are Michaelis and catalytic constants of PTEN and PI3K enzymes which catalyze the reactions of phosphorylation of phosphatidylinositol (PIP2) and dephosphorylation of phosphatidylinositol-3,4,5-trisphosphate (PIP3), respectively;  $K_{d,AKT}$  – dissociation constant of PIP3 binding with AKT.  $PTEN_o$ ,  $PI3K_o$ , and  $AKT_o$  are initial concentrations of the enzymes.

### 2.1.2. Sensitivity, resistance, and compensatory properties of the signalling network to RTK inhibitor

In our study of the sensitivity-to-resistance transition in the SN we use the following definitions of system sensitivity, resistance and compensation.

We define the sensitivity of the output signal, phospho-AKT (pAKT), of the whole HER2,3/PI3K/PTEN/AKT signalling network against RTK inhibitor, I, as:

$$S_{SN}(K, E_o, I, t) = \left| \frac{\Delta pAKT}{\Delta I} \right|, \quad (2)$$

which relates change in the response of output signal,  $\Delta pAKT$ , to changes in inhibitor concentration,  $\Delta I$ .  $S_{SN}$  depends on the kinetic parameters of the metabolites, enzymes, proteins and receptors  $K = k_1 \dots k_n$ , their initial concentrations  $E_o = e_1 \dots e_m$ , concentration of inhibitor  $I$ , and time after receptor stimulation,  $t$ . Here and below we consider the absolute value of sensitivity (vertical brackets in equation (2)).

In order to determine the relationship between sensitivity of the whole SN,  $S_{SN}$ , and the sensitivities of the receptor signalling system, RSS, and the signalling transduction system, STS, we use phospho-HER2 signal (pHER2) as the interconnector between RSS and STS as a surrogate of receptor activation since phosphorylation of HER2 occurs in response to receptor heterodimerization after ligand binding. We factorise  $S_{SN}$  (2) as follows:

$$S_{SN}(K, E_o, I, t) = \left| \frac{\Delta pAKT}{\Delta I} \right| = \left| \frac{\Delta pAKT}{\Delta pHER2} \frac{\Delta pHER2}{\Delta I} \right| \quad (3)$$

$$= S_{STS}(pHER2, K, E_o, t) \cdot S_{RSS}(I, K, E_o, t),$$

where

$$S_{RSS}(I, K, E_o, t) = \left| \frac{\Delta pHER2}{\Delta I} \right| \quad (4)$$

is the sensitivity of the receptor signalling system characterising the response of the output signal of RSS,  $\Delta pHER2$ , to a change in the input signal,  $\Delta I$ , and

$$S_{STS}(pHER2, K, E_o, t) = \left| \frac{\Delta pAKT}{\Delta pHER2} \right| \quad (5)$$

is the sensitivity of signalling transduction system, which is defined as the response of the output signal of STS,  $\Delta pAKT$ , to a change in the input signal of STS,  $\Delta pHER2$ .

Therefore, and in accordance with (3), the sensitivity of the whole SN,  $S_{SN}$ , depends on the sensitivities of both RSS,  $S_{RSS}$ , and STS,  $S_{STS}$ . This consideration of SN sensitivity,  $S_{SN}$  (3), relates to cases when an inhibitor targets the signal formed in the RSS (ErbB receptor system) and, in turn, this signal is transformed into the SN output signal through the STS (MAPK or PI3K/PTEN/AKT cascades). The specific properties of RSS and STS contributing to  $S_{RSS}$  and  $S_{STS}$  independently, and thus the  $S_{SN}$  overall, can be studied separately under this formulation.

As we will show below, the STS can be sensitive with one kinetic parameter set,  $K_a$ , but be insensitive with another set,  $K_b$ , for the same range in input signal pHER2. Such a change in sensitivity may arise from mutations that modify the kinetic parameters  $K$  and/or their initial concentrations,  $E_o$ , and these may manifest, for example, in acquired resistance to drug intervention. Likewise, the STS can be sensitive to one range in input signal, pHER2, and insensitive in another range in input signal for a given parameter set  $K$ . This could represent decreasing SN sensitivity in response to an increase in pHER2 signal due to overproduction of HER2 receptors.

We also distinguish between sensitivities in both RSS and STS subsystems to changes to a specific parameter  $p_i$  (i.e. one of the parameters in  $k_i$  and  $e_i$ ) of the proteins/receptors involved in the SN [36]:

$$S_{RSS,i} = \left| \frac{\Delta p_{HER2} / p_{HER2}}{\Delta p_i / p_i} \right|, \quad S_{STS,i} = \left| \frac{\Delta p_{AKT} / p_{AKT}}{\Delta p_i / p_i} \right| \quad (6)$$

The relative sensitivities  $S_{RSS,i}$  and  $S_{STS,i}$  (6) show respective relative responses  $\Delta p_{HER2}/p_{HER2}$  and  $\Delta p_{AKT}/p_{AKT}$  to relative change in the parameters,  $\Delta p_i / p_i$ . These relative sensitivities (6) are more suitable than absolute sensitivity ((2) - (5)) for the comparison of sensitivity across the range of different parameters as there is a wide range of values in this parameter set. In our computational calculation, the relative change applied to parameters for sensitivity analysis is always 0.1%. Below we analysed sensitivity values taken at time  $t=30$  min after HRG stimulation.

To analyse the sensitivity of SN to parameters  $p_i$  we also introduce the integrative sensitivity,  $S$ , as

$$S = \sum_{i=1}^N S_{STS,i} + S_{RSS,i}, \quad (7)$$

where  $N$  is the number of parameters (in  $k_i$  and  $e_i$ ) of the model.

We define acquired resistance to RTK inhibitor as the loss of sensitivity,  $S_{SN}$ , of the output signal pAKT to inhibitor concentration,  $I$  (2), in the defined region of physiological concentration of inhibitor close to its  $IC_{50}$ , i.e.,  $S_{SN} \cong 0$  in the resistance case. According to relation (3), resistance of SN to inhibitor  $I$  may arise from: 1) loss of sensitivity in RSS,  $S_{RSS} \cong 0$ , for example owing to HER2 receptor mutations or overexpression; 2) loss of sensitivity in STS,  $S_{STS} \cong 0$ , for example as a result of enzyme mutations in MAPK and/or PI3K/PTEN/AKT pathways. In our analysis (below), we determine the separate contributions of the sensitivities  $S_{RSS}$  and  $S_{STS}$  to the sensitivity of the whole SN,  $S_{SN}$ .

We define the compensatory features of the SN as the capability of the system to attenuate the effect of external perturbation, for example drug intervention, due to system-level regulation, for example feedback control or the changing of kinetic parameters,  $K$ , and/or expression levels,  $E_0$ , resulting from mutations [33]. In the case of drug resistance, compensatory mechanisms act to decrease network sensitivity and this can be treated as emerging robustness with respect to drug action [10,37]. We explore this sensitivity-to-resistance (robustness) transition below.

## 2.2. Experimental methods

### 2.2.1. Cell culture and collection of lysates

PE04 cells were routinely grown as monolayer cultures in DMEM supplemented with 10% heat-inactivated fetal calf serum (FCS) and penicillin/streptomycin (100 IU/mL) in a humidified atmosphere of 5% CO<sub>2</sub> at 37°C. Time course experiments were set up by plating cells into 10 cm Petri dishes, which were then left for 48 hours. Cells were washed briefly in PBS before transfer to phenol red-free DMEM containing 5% double charcoal-stripped serum supplemented with penicillin/streptomycin (100 IU/mL) and glutamine (0.3 mg/mL) for a further 48 h prior to treatment. Cells were treated with UCN-01 (protein kinase inhibitor; Calbiochem #539644; final concentration of 1 µM), LY294002 (PI3 kinase inhibitor; Calbiochem #440204; final concentration 20 µM), pertuzumab (HER2 inhibitor; final concentration 100 nM) and stimulation by heregulin (R&D Systems; 396-HB-CF) was at final concentration of 1 nM. Cells were treated for 15 minutes with the aforementioned drugs as appropriate immediately followed by the addition of heregulin-β (1 nM). The concentrations of drugs used in the experiments corresponded to the dose causing 50% inhibition of cell growth. Samples were collected at 60 minutes, washed in PBS, and immediately lysed in ice-cold isotonic lysis buffer [50 mM Tris-HCl (pH 7.5), 5 mM EGTA (pH 8.5), 150 mM NaCl, 1% Triton X-100] supplemented with aprotinin (10 µg/mL) and a protease inhibitor cocktail (Roche, 11836153001). Lysates were centrifuged for 6 min at 13,000 x g and protein concentrations of supernatants subsequently determined using the BCA assay (Sigma, BCA-1).

### 2.2.2. Western Blotting

Protein lysates were electrophoretically resolved on either 10% or 12% SDS-PAGE and transferred overnight onto Immobilon-P membranes (Millipore, Bedford, MA). After transfer, membranes were blocked with 1% blocking agent (Roche, #1520709) in TBS before probing overnight at 4°C with the appropriate primary antibody made up in 0.5% blocking agent. Primary antibodies used for western blotting were as follows: anti-phospho-AKT (Ser<sup>473</sup>) (Cell Signaling Technology, #9271) at 1:1000; anti-PTEN (Cell Signaling Technology, #9552) at 1:1000. Secondary antibody detection was performed with LiCor 1:10,000 IRdye680 (for the normalizer) and 1:10,000 of IRdye800 (for the target) for 45 minutes at room temperature in dark after which cells were washed in PBS, dried and then read on a Li-Cor Odyssey scanner at 680 nm and 780 nm.

### 2.2.3. *In cell Western Blotting*

PE04 cells were plated out in black 96-well round bottom trays and left for 24 hours after which they were washed in PBS and transferred to 5% double charcoal-stripped serum-containing media as described above. Following drug treatment, media was aspirated and cells were fixed in 100  $\mu$ L of 4% formaldehyde for 15 minutes at room temperature before being washed three times in PBS. Cells were permeabilized with 100  $\mu$ L of ice-cold methanol for 10 minutes at  $-20^{\circ}\text{C}$  and again washed in PBS. Staining was performed by blocking for 60 minutes at room temperature (5% goat serum / 0.3% Triton X-100 in PBS) after which primary antibody incubations (in 1% BSA / 0.3% Triton X-100 in PBS) were carried out overnight at  $4^{\circ}\text{C}$ . Antibodies to pAKT (Cell Signalling; #9271 at 1:50) and total AKT (Cell Signalling; #2920 at 1:50, were optimized for InCell western incubations. Secondary antibody detection was carried out as described for western blot analysis with 1:800 IRdye<sup>680</sup> (for the normalizer) and 1:800 of IRdye<sup>800</sup> (for the target). Analysis was carried out after pAKT : tAKT normalization.

## 3. Results

### 3.1. Signal response characteristics and the sensitivity-to-resistance transition in the receptor signalling system

To characterize the receptor signalling system, RSS, we studied the dose dependence of HER2 phosphorylation on two external signals, ligand (HRG) and drug (pertuzumab (2C4)), as well as on the concentration of HER2 receptors, which can vary for different cancer cell lines [18]. We also calculated the pAKT dose dependence on the same external signals to compare the responses of RSS and the whole SN.

The theoretical and experimental dependencies of pHER2 on the concentration of HRG, pHER2(HRG), and pertuzumab, pHER2(2C4), are shown in Figs. 2A and 2B respectively. The calculation of the dose response curve, pHER2(HRG), (see thick solid line in Fig. 2A) showed a switch-like behaviour of pHER2 signal at HRG stimulation: RTK activation from 10% to 100% occurs within a narrow range of HRG concentrations, and our experimental data showed saturation of pHER2 signal was achieved at 1 nM of HRG (see Fig. 2E). The best fit to the dose response curve pHER2(HRG) by the Hill function ( $\text{HRG}^n/(\text{HRG}^n+\text{K}^n)$ ), which characterises the steepness of this switch-like transition gives a Hill coefficient of  $n=2$ , and

this indicates cooperativity in the ligand/receptor complex formation and HER2/HER3 heterodimerization (see Fig. S1 in Supplement).  $EC_{50}$  obtained from theoretical dose dependence is consistent with experimental  $EC_{50}=3$  nM [16]. The pAKT dose response to HRG, pAKT(HRG), showed a switch-like behaviour similar to pHER2(HRG) (see thick dashed line in Fig. 2A). Maximal activation of AKT signal occurs within a narrow range of HRG concentration and its saturation is achieved at the concentration of HRG equal to 0.1 nM (see Fig. 2E). Thus both RSS and SN work in saturation mode at HRG concentration higher than 1 nM.

The dose dependences of the output signal of RSS, pHER2(2C4), and the output signal of SN, pAKT(2C4), on pertuzumab concentration (2C4) are shown in Fig. 2B (thick solid and dashed lines respectively). The difference between these output signals is determined by the inherent dose response characteristics of the STS (discussed in section 3.2). The inhibition of HER2 receptor by 100 nM pertuzumab causes 90% inhibition of RTK, pHER2 and 80% inhibition of pAKT (see experimental points on thick lines in Fig. 2B).

To model HER2 overexpression we increased 10-fold the concentration of HER2 receptor. Note that the initial HER2/HER3 ratio in the model equals 1.4, which is close to a recent experimental measure for the PE04 cell line (1.6) [18]. HER2 overexpression causes a shift in the pHER2 and pAKT dose dependences for pertuzumab to higher concentrations (see thin lines in Fig. 2B). This effect leads to an increase of approximately 200 times for pHER2  $EC_{50}$  and pAKT  $IC_{50}$ , and this 50% inhibition of pHER2 causes 10% inhibition of pAKT (see squares on thin lines in Fig. 2B). These results show that overexpression of HER2 causes insensitivity of the RSS and the whole SN to pertuzumab in the physiological range of pertuzumab concentrations (close to pertuzumab  $IC_{50}=40$  nM).

To study pHER2 and pAKT responses to pertuzumab in a wide range of HER2 expression levels, we calculated pHER2 and pAKT dose dependences on HER2 concentration in the presence and absence of 100 nM pertuzumab (see Fig. 2C). At HER2=100 nM the RSS and SN work in saturation mode in the absence of pertuzumab (see thick lines in Fig. 2C) and non-saturation mode in the presence of pertuzumab (see thin lines in Fig. 2C). With an increase in overexpression of HER2 by two orders of magnitude, RSS and SN return to function close to saturation mode in the presence of 100 nM of pertuzumab (see solid thin line at high concentrations of HER2 in Fig. 2C).

Note that in our model we do not consider the ligand-independent activation of HER2 due to HER2 homodimerization at HER2 overexpression [38], and focus on the HER2/HER3 activation of the PI3K/PTEN/AKT pathway. As a result, we propose that a 10-fold HER2

increase does not change the kinetics of receptor HER2/HER3 heterodimerization and the role of HER2 homodimerization in AKT activation is insignificant. Our calculation relates to the case of a lesser level of HER2 overexpression occurring through transcriptional/translational mechanisms without gene amplification [38]. An extension to our model is needed to describe and explain the effects of ligand independent activation of HER2 [38] on trastuzumab and pertuzumab resistance and anomalous phosphorylation of HER2 at the action of trastuzumab [39] and pertuzumab [40] at HER2 amplification.

To analyse the sensitivity of RSS to pertuzumab, we compared RSS sensitivities to the initial concentrations of receptors and their kinetic parameters,  $S_{RSS,i}$ , (6) in the absence and presence of 100 nM pertuzumab. As seen in Fig. 3, pertuzumab causes a noticeable increase in pHER2 sensitivity,  $S_{RSS,i}$ , to initial concentrations of HER2 and HRG (see white bars in Fig. 3A) as well as to almost all kinetic parameters  $k_i$  of the RSS (see white bars in Fig. 3B) compared to pHER2 sensitivity with no pertuzumab (black bars in Fig. 3A and B). This effect results from the transition of RSS kinetics from saturation to non-saturation mode due to HER2 inhibition by pertuzumab. In non-saturation mode the RSS becomes more sensitive to concentration of HER2 receptors and kinetic properties of receptors than in saturation mode.

The transition from non-saturation to saturation mode as a result of the increase of HER2 concentration was indicated by a reduction in pHER2 sensitivities,  $S_{RSS,i}$ , at pertuzumab action (see grey bars in Fig. 3A and B). Thus suppression of the pertuzumab inhibition effect from HER2 overexpression returns the pHER2 signal to the saturation region (see thin dashed line in Fig. 2B) and the sensitivity of the RSS to its initial low level. Note that the results of the sensitivity analysis of our model of the signalling in PE04 cells showed the dominant role of HER3 receptor in AKT signalling stimulated by HRG, where dominance is indicated by the size of the bar in Fig. 3A. This result is consistent with the results of sensitivity analysis of the model of AKT signalling in A431 [1] and ADRr cells [2] stimulated by HRG and so reflects the key role of HER3 receptor in HRG-induced AKT activation. The effects of pertuzumab and HER2 overexpression on the sensitivity  $S_{RSS,i}$  to HER3 concentration are slight because the pHER2 signal remains in saturation with respect to HER3 concentration in these cases (see Fig. 3A).

Our results showed the different dose responses of RSS and SN to pertuzumab (see thick lines pHER2(2C4) and pAKT(2C4) respectively in Fig. 2B). To analyse their mutual relationship, we calculated the sensitivities of RSS, STS, and the whole SN to pertuzumab,  $S_{RSS}$ ,  $S_{STS}$ , and  $S_{SN}$  (see Fig. 2D).  $S_{RSS}$  (4) and  $S_{SN}$  (2) were calculated based on the pHER2 and pAKT dose dependence for pertuzumab (see Fig. 2B);  $S_{STS}$  was derived from relation (3) as

$S_{STS} = S_{SN}/S_{RSS}$ . As shown, the sensitivity of the whole SN,  $S_{SN}$  (solid line in Fig. 2D), overlaps with  $S_{RSS}$  (dotted line in Fig. 2D) but shows more sensitivity at high pertuzumab concentrations. This difference between the sensitivities of SN and RSS is determined by the sensitivity of STS,  $S_{STS}$  (dashed line in Fig. 2D), and we analyse the properties of STS in detail.

### 3.2. Signal response characteristics and the sensitivity-to-resistance transition in the signal transduction system

To study the sensitivity-to-resistance transition in the signal transduction system, STS, we calculated the dependence of the output signal  $pAKT(pHER2, \gamma)$  on the input signal  $pHER2$  and control parameter  $\gamma$  (1). In Fig. 4A the dependence of  $pAKT(pHER2, \gamma)$  is shown for three characteristic values of  $\gamma$ :  $\gamma > 1$  – corresponding to suppression mode (dotted line);  $\gamma = 1$  – sensitive mode (solid line), and  $\gamma = 0.5$  – resistance mode (dashed line). The dependence of  $pAKT(pHER2, \gamma)$  for a wide range of  $pHER2$  and  $\gamma$  values is provided in Fig. S2 in Supplement.

We used the dependence  $pAKT(pHER2, \gamma)$  to profile  $pAKT$  signal changes in response to different perturbations of the STS: specifically inhibition of input signal by pertuzumab, so changing  $pHER2$  values; and PTEN, PI3K, and AKT mutations, so changing  $\gamma$ . For example, decreasing of  $pHER2$  from 1 to 0.1 due to RTK inhibition causes the decrease of  $pAKT$  signal from saturation value 1 to 0.2 at  $\gamma = 1$  (see tracking shown by arrow from initial state (1) to state (2) in Fig. 4A). The loss of PTEN activity effected by decreasing  $\gamma$  from 1 to 0.5 leads to restoration of the saturation of  $pAKT$  signal and confers pertuzumab resistance (see arrow from state (2) to state (3) in Fig. 4A).

Thus RTK inhibition transforms the functioning state of the STS from saturation to non-saturation mode, as depicted in the transition from initial state (1) to state (2). The functioning of the STS in non-saturation mode differs from when in saturation mode not only through the decreasing of  $pAKT$  signal but also through the increase in sensitivity of the STS to the input signal,  $pHER2$ . To show this, we calculated the dependence of sensitivity  $S_{STS}$  (5) on  $pHER2$  concentration and  $\gamma$  30 minutes after HRG stimulation (see Fig. 4B). We profiled the same trajectory (1-2-3) as shown in Fig. 4A. A decrease in  $pHER2$  signal as a result of RTK inhibition causes sensitivity  $S_{STS}$  to increase by approximately 50 times (transition (1-2) in Fig.

4B). The PTEN loss leading to saturation restoration, effected through decreasing  $\gamma$  results in reducing  $S_{STS}$  sensitivity to its initial low level (transition (2-3) in Fig. 4B).

The increase in  $S_{STS}$  observed at low pHER2 signals (see states (2) in Figs. 4A and B) is a result of the transition from saturation to non-saturation mode at the inhibition of pHER2 signal. In addition to the increase of  $S_{STS}$ , we expect an increase in the sensitivities  $S_{STS,i}$  (6) to kinetic parameters,  $k_i$ , and initial protein concentrations,  $e_i$ . To study this effect we calculated  $S_{STS,i}$  (6) under different perturbations of the STS that induce this transition (see Figs. 5A and B). As seen, pHER2 inhibition by pertuzumab increases sensitivity  $S_{STS,i}$  to the kinetic parameters of the reactions in PI3K/PTEN/AKT cycle and AKT phosphorylation reactions [32] (black and white bars in Fig. 5A and B, respectively). The increase in sensitivities  $S_{STS,i}$  (6) to  $k_i$  and  $e_i$  occurs when the pertuzumab concentration is in its  $IC_{50}$  range and where sensitivity  $S_{STS}$  to pHER2 signal increases.

A reverse in sensitivities  $S_{STS,i}$  (6) was observed when effecting the sensitivity-to-resistance transition in the PI3K/PTEN/AKT pathway at the loss of PTEN activity through PTEN inhibition by bpV(pic) [41] (see grey bars in Figs 5A and B), where sensitivities are significantly reduced compared with their increased levels at pertuzumab action alone (white bars). Note, the same reverse in sensitivities of STS parameters may be obtained by changing PI3K and AKT activities, corresponding to *PIK3CA* mutations and AKT overexpression respectively (see Fig. S3 in Supplement). Thus the sensitivity-to-resistance transition in the PI3K/PTEN/AKT pathway occurs with the restoration of both saturation level of pAKT signal and low values of sensitivities  $S_{STS,i}$  to kinetic parameters and initial levels of enzyme expression.

The mechanism underlying the decrease in  $S_{STS,i}$  at low  $\gamma$  (resistance mode) is determined by the saturation of PIP3 production as result of the imbalance of the enzyme activities in the PI3K/PTEN/AKT cycle: this imbalance leads to the restoration of saturation in the reaction of PIP3 binding with AKT (see next section for further analysis). Note that in normal functioning of the SN the concentration of PIP3 is not in saturation and the PIP2/PIP3 balance, as controlled by the PI3K/PTEN/AKT cycle, provides the STS with a regulation mechanism [33].

To study the correlation between overall sensitivity changes in the STS and different perturbations to PI3K/PTEN/AKT cycle we calculated integrated sensitivity  $S$  (7) and compared it with observed experimental levels of pAKT inhibition by different inhibitors and their combinations (pertuzumab; inhibitor of PI3K, LY294002; pertuzumab+bpV(pic);

pertuzumab+LY294002) (see Fig. 5E). pAKT inhibition is attended by an increase in sensitivity in the presence of either pertuzumab (bars 2) or LY294002 (bars 4) or pertuzumab+LY294002 (bars 5) with respect to the control (bars 1). Resistance to pAKT inhibition occurring in conjunction with a decreasing in  $S$  is shown in the resistance effect of bpV(pic) when combined with pertuzumab (bars 3). These theoretical and experimental results show that the sensitivity of the STS to RTK inhibition, kinetic parameters and expression levels of proteins is under the control of the PTEN/PI3K/AKT cycle. We thus propose that the sensitivity of the STS, and so the SN as a whole, to RTK inhibition can be controlled by manipulation of the activity of the PTEN/PI3K/AKT cycle.

### 3.3. Controlling sensitivity through the PTEN/PI3K/AKT cycle

We have shown that an increase in sensitivity  $S_{SN}$  to inhibitors is attended to by an increase in sensitivity  $S_{STS,i}$  to the kinetic parameters of the proteins and their expression levels. This means that sensitive SNs may be more fragile with respect to mutations that change protein kinetic properties (dissociation or/and catalytic constants) and protein abundance. In particular, an increasing sensitivity would appear to be an adverse effect of inhibitor action since a high sensitivity endows the SN with fragility with respect to mutations that compensate for inhibitor effect by restoring the initial low sensitivity and high output signal of the SN, and it is thus desirable to effect inhibition without changing SN sensitivity.

As seen from the calculation of pAKT dose response and sensitivity depending on pHER2 signal and parameter  $\gamma$  (see Fig. 4A and B), we can reach a state of high inhibition of pAKT (2\*) and low sensitivity (see trajectory (1-2\*) in Figs 4A and B). This state (2\*) can be obtained by RTK inhibition by pertuzumab (decrease of pHER2 signal) when increasing  $\gamma$ . One of the ways to achieve a high  $\gamma$  value is to decrease PI3K activity through its inhibition (see equation (1) and [33]). In Fig. 4A and B we profiled RTK inhibition of the pHER2 signal followed by the transition from one dose response curve ( $\gamma=1$ ) to another ( $\gamma>1$ ) at inhibition of PI3K by 1  $\mu\text{M}$  of LY294002. This combination of RTK and PI3K inhibition leads to the state (2\*) with a sensitivity close to the unperturbed state (1) and high level of pAKT inhibition. Note that low sensitivity at low pHER2 signal is achieved due to the sigmoid form of the dose response curve pAKT(pHER2), which is more visible at higher  $\gamma$  (see Fig. 4A).

The sigmoid form of the dose response curve pAKT(pHER2) also affords a state of low sensitivity with a high inhibition (see state (4) in Fig. 4A and B). We suggested that this high

inhibition level of RTK can be reached by inhibition of HER2/HER3 heterodimerization by combination of trastuzumab and pertuzumab [40,42] or HER2 inhibitor combined with small molecular RTK inhibitors [17].

### 3.4. Post-translation modification of PTEN and sensitivity-to-resistance transition due to CK2/GSK3 amplification

In section 3.2 we analysed the sensitivity-to-resistance transition in the PI3K/PTEN/AKT pathway resulting from PTEN inactivation, which can arise from *PTEN* aberrant expression or deletion mutation [27]. Here we analyse another mechanism for loss of PTEN activity, due to post-translation regulation of PTEN [22]. It is known that PTEN is under the control of casein kinase 2 (CK2) and glycogen synthase kinase 3 $\beta$  (GSK3 $\beta$ ), which inactivate PTEN as a result of direct phosphorylation of the PTEN C-terminal domain [22].

In the model, we took into account the PTEN/pPTEN cycle, and PTEN phosphorylation by CK2 and GSK3 $\beta$  enzymes is modelled by one phenomenological reaction (CK2/GSK3 $\beta$  reaction in Fig. 1). pPTEN dephosphorylation is assumed to be catalysed by PTEN due to its weak protein phosphatase activity [22]. Experimental data on phosphorylation of PTEN during AKT activation was obtained in our experiments in PE04 cells [32] and in breast cells KPL-1 [43]. In the model, accumulation of pPTEN results from lowering the reaction rate of pPTEN dephosphorylation due to a decrease in the free PTEN level in the cytoplasm when signalling. We suggested that production of membrane PIP3 induced by PI3K activation causes PTEN relocation from the cytosol to the plasma membrane and that decreases dephosphorylation of pPTEN [22,44].

*In silico* experiments showed that a further increase in the inactive form of PTEN (pPTEN) occurs at the overexpression of CK2 or GSK3 $\beta$  kinases (see Fig. S4A in Supplement). As a result, the imbalance in enzyme activities in the PI3K/PTEN/AKT cycle can effect the sensitivity-to-resistance transition in the SN. The pAKT dose-dependence for pertuzumab calculated at a 3-fold increase in activity of CK2/GSK3 $\beta$  reaction confirmed this (see dotted line in Fig. 2B). Amplification of the CK2/GSK3 $\beta$  reaction leads to a shift of pertuzumab IC<sub>50</sub> by a factor of approximately 100 and thus insensitivity to pertuzumab at its physiological concentrations.

Thus activation of the AKT signal may occur at the normal expression of PTEN, but at aberrant PTEN regulation in the PTEN/pPTEN cycle due to overexpression of CK2 and/or

constitutive expression of GSK3 $\beta$ . Experimentally, it was observed that hyperactivation of the PI3K/PTEN/AKT pathway was induced by overexpression of CK2 in lymphoblastic leukaemia cells [45] and by overexpression of GSK3 $\beta$  in an ovarian carcinoma cell line [46].

While CK2/GSK3 $\beta$  overexpression can effect the sensitivity-to-resistance transition, the inhibition of CK2/GSK3 $\beta$  kinases can reverse this transition and suppress resistance against RTK inhibitor resulting from the loss of PTEN activity. Modelling the effect of pertuzumab at the loss of PTEN activity and inhibition of PTEN phosphorylation showed particular suppression of resistance and restoration of sensitivity to pertuzumab (see Fig. 6B (lines)).

We also observed that CK2/GSK3 $\beta$  overexpression brings about the same change in sensitivities  $S_{STS,i}$  as in the case of the direct loss of PTEN activity (see section 3.2). CK2/GSK3 $\beta$  overexpression causes a reduction in those sensitivities that were increased as a result of pertuzumab action (see Fig. S4B in Supplement). The mechanism of this effect is identical to that of the direct loss of PTEN activities: CK2/GSK3 $\beta$  overexpression leading to PTEN inactivation restores saturation mode in the PI3K/PTEN/AKT cycle perturbed by pertuzumab.

### 3.5. PTEN loss and the efficacy of the target inhibition in PTEN upstream and downstream pathways

The identification of optimal drug targets to inhibit effectively pathway output signals in cancer cells is made especially challenging by observed *de novo* or acquired activating mutations in signalling pathways, and SN dynamics under mutations are further impacted on by complex feedback loops that regulate pathway activation [10,13,21,37,47]. We illustrate this problem by considering the effect of PTEN loss on inhibition efficacy of the targets in PTEN upstream and downstream pathways.

With regard to the upstream pathway, we have shown that PTEN loss changes the SN response to inhibition of targets: specifically the pAKT output signal becomes insensitive to HER2 inhibition because of a perturbation to the balance of enzyme activities in the PI3K/PTEN/AKT cycle by the loss PTEN activity ( $\gamma < 1$ ) [32, 33]. A combination of HER2 inhibition together with inhibition of another target in the PTEN upstream module, PI3K enzyme, can overcome resistance to HER2 inhibitor at PTEN loss [28,33]. This effect is due to restoration of the enzyme activity balance in the PI3K/PTEN/AKT cycle by PI3K inhibition ( $\gamma = 1$ ) that then restores the initial response of the pAKT signal to HER2 inhibition [33].

Here we analyse the influence of PTEN loss on the PTEN downstream pathway and the efficacy of target inhibition in this pathway. In the model, PTEN inhibition leads to a two-fold increase in PIP3 concentration [33], and this can change the pAKT signal due to the positive loops of activation of downstream enzymes, AKT and PDK1. It is known that PIP3 lipids induce translocation of AKT and PDK1 enzymes to the plasma membrane from the cytosol and their activation when binding with PIP3 [48]. This positive loop of activation of PTEN downstream reactions may cause further AKT activation at PTEN loss.

Our experiments with inhibition of PTEN by bpV(pic) showed no noticeable effect of PTEN inhibition on HRG-induced AKT activation in PE04 cells (see Fig. 6A and [32]). To analyse this result we calculated the pAKT dependence on PTEN concentration; similarly there was little observed effect of PTEN activity on pAKT signal at saturated HRG signal up to normal PTEN concentrations in the model, 40-50 nM (see solid line in Fig. 6B) and this accords with experimental data (see bars 1 and 5 in Fig. 6C). We conclude that this higher level of PIP3 does not influence the saturated level of active pAKT (AKT-PIP3 complex) reached at uninhibited PTEN. Thus, the concentration of AKT enzyme is a rate-determining factor in the activation of AKT by PIP3 in PE04 cells. Note that this effect depends on the relationship of synthesized PIP3 and initial AKT concentrations which can differ for different cell lines [48].

Another consequence of PTEN loss, and following an increase in PIP3 level, is PIP3-induced translocation of PDK1 enzyme to the plasma membrane from the cytosol and its activation by PIP3 [48]. Our experiment on PTEN inhibition did not show any pAKT increase as a result of PIP3-induced activation of PDK1 (see Fig. 6A), and so analysis of pAKT level does not reveal the relation between the level of PDK1 activation and the increased level of PIP3. At pAKT saturation, independent of the level of PIP3, PIP3-induced activation of PDK1 may only cause an increase in the rate of AKT phosphorylation without affecting its level at saturation. The extent of PIP3-induced activation of PDK1 arising from PTEN loss can be tested by comparison of the inhibition effects of PDK1 at the different activities of PTEN.

Our experiments showed that for normal PTEN activity, it is possible to inhibit by approximately 90% the pAKT signal in PE04 cells at saturated HRG signal. This may be through upstream (RTK) inhibitor (Fig. 5E, bar 2), downstream PDK1 inhibition with UCN-01 [49] (Fig. 6C, bar 3), or the combination of RTK and UCN-01 inhibitors (Fig. 6C, bar 4). In contrast, in our experiments where PTEN activity is lost by bpV(pic) action, it is not possible to inhibit the pAKT signal: neither RTK inhibitor (Fig. 5E, bar 3) nor the

combination of RTK and UCN-01 inhibitors (Fig. 6C, bar 5) has any significant effect on the saturated pAKT signal.

Thus our experiment showed that increasing activity of PDK1 due to the increase in the local concentration of active PDK1 reduces efficacy of PDK1 inhibition at PTEN loss in PE04 cells. Therefore, in contrast to the inhibition of PI3K in the PTEN upstream pathway, the inhibition of PDK1 in the PTEN downstream pathway at PTEN loss did not restore the inhibition effect of pertuzumab in PE04 cells, and this was due to the PIP3-induced activation loop in PTEN downstream pathway [48].

### 3.6. PTEN-dependent and independent activation of AKT

As discussed above, our *in silico* and *in vitro* experiments showed independence of pAKT signal on PTEN activity at saturated receptor signal in PE04 cells (see solid line in Fig. 6B). By contrast, we also observed PTEN-dependent activation of AKT at non-saturated receptor signals at its inhibition by pertuzumab (see dashed line in Fig. 6B). The theoretical dependence of pAKT on PTEN concentration at HER2 inhibition showed an increase in pAKT signal at a decrease in PTEN concentration until pAKT saturation. Our experiments confirmed reciprocal dependence of pAKT level on PTEN activity at its inhibition by pertuzumab in PE04 cells [32]. Based on our modelling, we showed that PTEN loss causes amplification of non-saturated pHER2 signal up to saturated pAKT signal that leads to resistance to HER2 inhibition [32,33].

A similar reciprocal PTEN-dependent activation of AKT was observed in our *in vitro* experimental data on the dependence of constitutive AKT activation on PTEN expression level in 13 ovarian cancer cell lines (see experimental points (squares) in Fig. 6B and cell lines characteristics in [32]). Likewise, a negative correlation between pAKT and PTEN expression was obtained in basal-like breast carcinoma (but not HER2+ carcinoma) [28] (experimental points (circles) in Fig. 6B) and other cancers [24]. Linking our theoretical results obtained at non-saturated receptor signal and experimental data on PTEN-dependent activation of AKT (see Fig. 6B) we suggested that constitutive AKT activation in cancer cells may be induced by weak non-saturated mitogenic signal and amplified to saturated pAKT level as a result of PTEN loss. Otherwise, variation in PTEN expression at saturated mitogenic receptor signals would not impact pAKT level, as shown in our results on PTEN-independent activation (solid line in Fig. 6B). Note that our modeling showed that

amplification of a weak non-saturated mitogenic signal may also result from activating mutations of other enzymes such as PI3K or AKT [33].

In summary, we conclude that the effect of PTEN loss on AKT activation depends on the level of receptor signal. PTEN-independent activation of AKT is observed at saturated HRG signal and PTEN-dependent activation of AKT is observed at non-saturated receptor signals (for example, at receptor inhibition or weak receptor stimulus). Thus the consequences of PTEN loss only manifest at non-saturated receptor signal by amplification of a low pHER2 signal up to a saturated pAKT signal.

## Discussion

*Receptor signalling system functioning in response to HER2 inhibition and overexpression.* We explored, through *in vitro* and *in silico* experiments based on the ovarian cancer cell line PE04, the whole signalling network response to HRG stimulation. We observed that the output signal, pAKT, was saturated with respect to HRG at concentrations greater than 0.1 nM. Likewise a pAKT saturation regime has been observed in the PDGF/PI3K/AKT signalling pathway in fibroblasts [34], and it was suggested that the saturated pAKT signal is insensitive to ligand concentration and more sustained in relation to receptor phosphorylation. Our results accord with this: sensitivity of the SN output signal to variation in input signal and receptor kinetic parameters is minimal when the SN functions in saturation regime. However, sensitivity increases when SN is not in this saturation regime, for example at HRG concentrations less than 0.01 nM. To explore this phenomenon in detail we considered the sensitivity of the receptor signalling system, RSS.

As with the SN, the RSS output signal, pHER2, is saturated at HRG concentrations greater than 0.1 nM. HER2 inhibitor effects the transition of RSS from saturation to non-saturation mode and changes both inhibited response and increased sensitivity to external and internal perturbations to the RSS. Our results of modelling HER2 overexpression confirmed that increasing HER2 expression is one of the main mechanisms underlying resistance to HER2 inhibitors in the RSS. We showed that HER2 overexpression leads to restoration of the saturated RTK signal and a consequent decrease in sensitivity to HER2 inhibition at its physiological concentrations. Our experimental data showed that pertuzumab efficacy to inhibit AKT activation and cell growth rate fell dramatically in cell lines with high level of

HER2 expression with respect to HER3, i.e., ovarian cancer cell lines OAW42 and SKOV3 [18].

The signal responses of the SN and RSS to HRG stimulation are similar, with the two dose dependences having close  $EC_{50}$ s and reaching saturation over a narrow range of ligand concentrations, which indicates activation of the SN in PE04 cells occurs at the same range of ligand concentrations as RSS activation. Specifically, we observed a switch-like response to HRG activation in both SN and RSS. More generally, the comparison of receptor system and whole network responses to receptor activation showed different behaviours. For example, while similar switch-like behaviours were observed in PDGF/PI3K/AKT signalling in fibroblasts [3,34] and some cancer cell lines [1], in other cancer cell lines the pAKT dose dependence on EGF concentration was observed to have log-linear behaviour with  $EC_{50}$ s less by a factor of 0.01 to 0.1 than the receptor response to EGF [1]. To explain the switch-like behaviour, Perk et al. [34] proposed that the underlying mechanism is cooperative receptor dimerization.

Notably, the response of the whole PI3K/PTEN/AKT signalling network in different cells shows more diversity in whole network response than receptor response to receptor activation [1]. This diversity is most likely a consequence of the dependence of the response of the signal transduction system to different expression levels of the proteins involved in STS of different cells.

*Sensitivity-to-resistance transitions through mutations in the signal transduction system:* The response of the signal transduction system (STS), pAKT, to input signal, pHER2, showed that the form of the response depends on the PI3K/PTEN/AKT pathway control parameter,  $\gamma$ , and ranges from switch-like behaviour at low  $\gamma$  (hypersensitivity) to smooth sigmoid response at  $\gamma=1$  (sensitivity) to suppression behaviour at  $\gamma>1$  (see Fig. 4A). This behaviour, obtained for PE04 cells, differs from that obtained in PDGF/PI3K/AKT signalling in fibroblasts [34] where the receptor-signal response curve pAKT(pPDGF) was hyperbolic in form without any sigmoid features (see comparison of two response curves in Fig. S5 in Supplement). While this receptor-signal response curve varies among cell lines [1], we propose that it is possible to control the sensitivity-to-resistance transition through perturbations to the STS. To demonstrate this, we explored a range of PI3K/PTEN/AKT pathway perturbations.

Loss of PTEN activity results in a shift in the STS signal response (pAKT) to HRG to lower HRG concentrations (dotted line, Fig. 2A), and the  $EC_{50}$  for pAKT dose dependence decreased by approximately one order of magnitude relative to  $EC_{50}$  for pHER2. Note that the same shift was observed in other cancer cells [1]. PTEN loss thus causes hypersensitivity in

the STS leading to AKT activation by extremely low receptor signal (0.001 nM) and saturation at 5% activation of HER2 phosphorylation in PE04 cells. The PTEN-induced hypersensitivity of STS was caused by the transition from non-saturation to saturation in the PIP2/PIP3 cycle, which is controlled by the balance of PI3K, PTEN, and AKT enzyme activities [33]. To study the role of PTEN level in the regulation of PIP3 pool and AKT activation we carried out *in vitro* experiments on PTEN inactivation in PE04 cells. The experiments showed no noticeable effect of PTEN inhibition on AKT activation (see Fig. 6A). Thus, the excessive level of PIP3 induced by PTEN inhibition does not influence the saturated level of active AKT; concentration of AKT enzyme is a rate-determining factor in AKT activation by PIP3, confirming the suggestion that a low level of PIP3 is sufficient for AKT activation [34]. Further, the dominant role of initial concentration of AKT in output response of PE04 cells was shown through sensitivity analysis (see Fig. 5C) and this agrees with results of sensitivity analysis for A431 [1] and ADRr cells [2].

*In silico* and *in vitro* experiments in PE04 cells showed that the consequences of perturbations to the PI3K/PTEN/AKT cycle depend on receptor signal level. For saturated HRG concentrations, PTEN loss does not affect AKT activation; for non-saturated HRG, PTEN loss causes AKT activation in the PTEN downstream pathway and SN resistance to upstream inhibition. Thus, the sensitivity-resistance transition occurs due to PTEN-dependent activation of AKT at HER2 inhibition. The same PTEN-dependent activation was observed in experimental data on 13 ovarian cancer cell lines (see Fig. 6B). We represented the effect of PTEN loss, together with PI3K mutation and CK2/GS3 $\beta$  overexpression, on the SN by the frames shown in Fig. 1 (frames 1, 2, and 3 respectively). As this effect depends on the level of receptor signal, frames 1, 2, and 3 (absence of HER2 inhibitor) extend only over a small part of the pathway, whereas frames 1a, 2a, and 3a (presence of HER2 inhibitor) show that the influence of the PI3K/PTEN/AKT perturbation extends to the downstream pathway. Note, our mapping of the effect of PTEN loss, PI3K mutation and CK2/GSK3 $\beta$  overexpression are restricted to a small part of the downstream pathway of PI3K/PTEN/AKT signalling and does not include other PIP3-dependent processes [50]. This mapping summarizes our analysis of the mutation-induced perturbations in upstream and downstream pathways of the signalling network and can inform identification of optimal drug targets for single and combination anti-cancer therapy.

*Preserving sensitivity of SN to mutations with combined drug interventions on the PI3K/PTEN/AKT pathway:* We suggest that drug interventions that increase SN sensitivity to

external perturbations, e.g., HER2 inhibition, endow that SN with fragility with respect to mutations that abrogate the inhibition effect of drug. Such mutations may alter kinetic properties of key proteins and their expression levels, and may restore initial saturation with maximal output signal and significantly lower sensitivity to drug action (cancer robustness). We demonstrated SN fragility and acquired robustness with a combination of two inhibitors (UCN-01 and pertuzumab) possessing high efficacy that loses efficacy after SN mutation, here PTEN loss, which lowers SN sensitivity. It is thus attractive in the context of combination therapy to inhibit AKT activation without increasing SN sensitivity and to prevent cells from acquired mutations compensating for drug effect.

We showed that the increase in SN sensitivity induced by HER2 inhibition can be prevented by the combination of HER2 inhibition and PI3K inhibition. *In vitro* experiments demonstrated the effectiveness of a combined pertuzumab and PI3K inhibitor (LY294002) in the prevention of pertuzumab resistance at PTEN loss in PE04 cells [33]. Moreover SN sensitivity induced by HER inhibition correlates with the unique capability of RTK inhibitors to sensitise cancer cells to cytotoxic drugs [8]. For example, the effect of the increase in sensitivity to the additional drug (docetaxel) was observed at the inhibition of HER receptors by cetuximab, trastuzumab, or pertuzumab in human ovarian cancer cell lines [51].

We explored the impact of upstream and downstream interventions, with PTEN loss as an example. We compared experimental results of inhibition of PI3K in the PTEN upstream pathway with PDK1 inhibition in the PTEN downstream pathway, and showed that upstream inhibition abrogated resistance to pertuzumab more effectively than downstream inhibition. This difference in inhibition performance was suggested to arise from an activation loop induced in the downstream pathway by PTEN loss. These results demonstrate the consequence of mutations, which can significantly change the effect of drugs targeting upstream and downstream pathways.

## Conclusions

The response of AKT activation to HER2 inhibitor was studied theoretically and experimentally by manipulation of the receptors and enzymes activities involved in the PI3K/PTEN/AKT signalling network in the PE04 ovarian cancer cell line. This perturbation technique permitted us to model different changes in the signalling network typical in cancer development, anticancer therapy, and drug resistance. In *in silico* and *in vitro* experiments, we

modeled sensitive and resistant modes in the signalling network, and observed the sensitivity-to-resistance transition for different perturbations of the PI3K/PTEN/AKT pathway. Analysis of sustained activation of AKT by HRG in the absence of HER2 inhibition showed that most modules of the HER2,3/PI3K/PTEN/AKT pathway function in saturation with respect to HRG signal. We suggested that the saturation mode of activation kinetics endows the SN with robustness to fluctuation of the external signal as well as internal perturbations induced by mutations.

Sensitivity analysis of AKT activation at HER2 inhibition showed that drug action significantly increased sensitivity of the response to external signal and perturbations of the internal properties of the SN. This effect results from that HER2 inhibitor causes the transition of signaling system from saturation to non-saturation mode. In *in silico* modeling of the mutation effects on SN sensitivity at anti-HER2 drug action showed that PTEN loss, PI3K mutations, and AKT and GSK3 $\beta$ /CK2 overexpression lower SN sensitivity since the system returns to saturation mode. Based on these results, we suggested that the drug-induced increase of SN sensitivity to internal perturbations leads to SN fragility with respect to mutations that compensate for drug effect through the sensitivity-to-resistance transition. Moreover, the increase in SN sensitivity at HER2 inhibition promotes using combined inhibition leading to the synergetic effect of two inhibitors. However, the efficacy of combined inhibitors can be suppressed by specific mutations in the SN. For example, through PTEN loss we demonstrated that the efficacy of AKT inhibition depends on the choice of the inhibitor target: either PTEN upstream or downstream pathways. Thus, drug target identification for combination anti-cancer therapy needs to account for the mutation effects on the upstream and downstream pathways.

## Acknowledgments

This work was supported by grants from Breakthrough Breast Cancer and Scottish Funding Council (SRDG), and personal support to AG from Scottish Informatics and Computer Science Alliance (SICSA).

## References

- [1] W.W. Chen, B. Schoeberl, P.J. Jasper, M Niepel, U.B. Nielsen, D.A. Lauffenburger, P.K. Sorger, *Mol. Syst Biol.* 5 (2009) 239.

- [2] B. Schoeberl, E.A. Pace, J. B. Fitzgerald, B.D. Harms, L. Xu, L. Nie, B. Linggi, A. Kalra, V. Paragas, R. Bukhalid, V. Grantcharova, N. Kohli, K. A. West, M. Leszczyniecka, M. J. Feldhaus, A. J. Kudla, U. B. Nielsen, *Sci. Signal.* 2 (2009) ra31.
- [3] C.C. Wang, M. Cirit, J.M. Haugh, *Mol. Syst. Biol.* 5 (2009) 246.
- [4] M.R. Birtwistle, M. Hatakeyama, N. Yumoto, B.A. Ogunnaike, J.B. Hoek, B.N. Kholodenko, *Mol. Syst. Biol.* 3 (2007) 144.
- [5] D.A. Lauffenburger, *Carcinogenesis* 31 (2010) 2.
- [6] D. Faratian, R.G. Clyde, J.W. Crawford, D.J. Harrison, *Nat. Rev. Clin. Oncol.* 6 (2009) 455.
- [7] D. Faratian, J.L. Bown, V.A. Smith, S.P. Langdon, D.J. Harrison, *Methods Mol. Biol.* 662 (2010) 245.
- [8] E. Klipp, R.C. Wade, U. Kummer, *Curr. Opin. Biotechnol.* 21 (2010) 511.
- [9] T. Shiraishi, S. Matsuyama, H. Kitano, *PLoS Comput. Biol.* 6 (2010) e1000851.
- [10] H. Kitano, *Nat. Rev. Drug Discov.* 6 (2007) 202.
- [11] A.C. Faber, D. Li, Y.C. Song, M.C. Liang, B.Y. Yeap, R.T. Bronson, E. Lifshits, Z. Chen, S. Maira, C. García-Echeverría, K.K. Wong, J.A. Engelmann, *Proc. Natl. Acad. Sci. U S A.* 106 (2009) 19503.
- [12] T.L. Yuan, L.C. Cantley, *Oncogene.* 272 (2008) 5497.
- [13] I. Amit, R. Wides, Y. Yarden, *Mol. Syst. Biol.* 3 (2007) 151.
- [14] E. Aksentijevic, B.N. Kholodenko, W. Kolch, J.B. Hoek, A. Kiyatkin, *Cell. Signal.* 22 (2010) 1369.
- [15] J.A. McCubrey, M.L. Sokolosky, B.D. Lehmann, J.R. Taylor, P.M. Navolanic, W.H. Chappell, S.L. Abrams, K.M. Stadelman, E.W. Wong, N. Misaghian, S. Horn, J. Bäsecke, M. Libra, F. Stivala, G. Ligresti, A. Tafuri, M. Milella, M. Zarzycki, A. Dzugaj, F. Chiarini, C. Evangelisti, A.M. Martelli, D.M. Terrian, R.A. Franklin, L.S. Steelman, *Adv. Enzyme Regul.* 48 (2008) 113.
- [16] M.C. Franklin, K.D. Carey, F.F. Vajdos, D.J. Leahy, A.M. de Vos, M.X. Sliwkowski, *Cancer Cell.* 5 (2004) 317.
- [17] G. Giamas, Y.L. Man, H. Hirner, J. Bischof, K. Kramer, K. Khan, S.S. Ahmed, J. Stebbing, U. Knippschild, *Cell. Signal.* 22 (2010) 984.
- [18] Y. Nagumo, D. Faratian, P. Mullen, D.J. Harrison, M. Hasmann, S.P. Langdon, *Mol. Cancer Res.* 7 (2009) 1563.
- [19] S.P. Langdon, D. Faratian, Y. Nagumo, P. Mullen, D.J. Harrison. *Expert. Opin. Biol. Ther.* 10 (2010) 1113.

- [20] C.F. Singer, W.J. Köstler, G. Hudelist, *Biochim. Biophys. Acta* 1786 (2008) 105.
- [21] J.A. Engelman, J. Settleman, *Curr. Opin. Genet. Dev.* 18 (2008) 73.
- [22] N.R. Leslie, C.P. Downes, *Biochem. J.* 382 (2004) 1.
- [23] J.A. Engelman, *Nat. Rev. Cancer* 9 (2009) 550.
- [24] K. Stemke-Hale<sup>1</sup>, A.M. Gonzalez-Angulo<sup>1</sup>, A. Lluch, R.M. Neve, *Cancer Res.* 68 (2008) 6084.
- [25] K. Berns, *Cell* 12 (2007) 395.
- [26] C. Liedtke, L. Cardone, A. Tordai, K. Yan, H.L. Gomez, L.J. Figureoa, R.E. Hubbard, V. Valero, E.A. Souchon, W.F. Symmans, G.N Hortobagyi, A. Bardelli, L. Pusztai, *Breast Cancer Res.* 10 (2008) R27.
- [27] Y. Nagata , K.H. Lan , X. Zhou , M. Tan , F.J. Esteva , A.A. Sahin , K.S. Klos , P. Li , B.P. Monia , N.T. Nguyen , G.N. Hortobagyi , M.C. Hung , D. Yu, *Cancer Cell.* 6 (2004) 117.
- [28] B. Marty, V. Maire, E. Gravier, G. Rigai, A. Vincent-Salomon, M. Kappler, I. Lebigot, F. Djelti, A. Tourdès, P. Gestraud, P. Hupé, E. Barillot, F. Cruzalegui, G.C. Tucker, MH Stern, J.P. Thiery, J.A. Hickman, T. Dubois, *Breast Cancer Res.* 10 (2008) R101.
- [29] G. Pérez-Tenorio, L. Alkhori, B. Olsson, M.A. Waltersson, B. Nordenskjöld, L.E. Rutqvist, L. Skoog , O. Stål, *Clin. Cancer Res.* 13 (2007) 3577.
- [30] L.H. Saal, K. Holm, M. Maurer, L. Memeo, T. Su, X. Wang, J.S. Yu, P.O. Malmström, M. Mansukhani, J. Enoksson, H. Hibshoosh, A. Borg, R. Parsons, *Cancer Res.* 65 (2005) 2554.
- [31] N.A. O'Brien, B.C. Browne, L. Chow, Y. Wang, C. Ginther, J. Arboleda, M.J. Duffy, J. Crown, N. O'Donovan, D.J. Slamon, *Mol. Cancer Ther.* 9 (2010) 1489.
- [32] D. Faratian, A. Goltsov, G. Lebedeva, S. Moodie, P. Mullen, C. Kay, I. H. Um, S. Langdon, I. Goryanin, D.J. Harrison, *Cancer Res.* 69 (2009) 6713.
- [33] A. Goltsov, D. Faratian, S.P. Langdon, J. Bown, I. Goryanin, D.J. Harrison, *Cell. Signal.* 23 (2011) 407.
- [34] C.S. Park, I.C. Schneider, J.M. Haugh, *J. Biol. Chem.* 278 (2003) 37064.
- [35] A.M. Martelli, I. Faenza, A.M. Billi, L. Manzoli, C. Evangelisti, F. Falà, L. Cocco, *Cell. Signal.* 18 (2006) 1101.
- [36] Z. Zi, Y. Zheng, A.E. Rundell, E. Klipp, *BMC Bioinformatics.* 9 (2008) 342.
- [37] H. Kitano, *Nat. Rev. Cancer.* 4 (2004) 227.
- [38] J.W. Park, R.M. Neve, J. Szollosi, C.C. Benz, *Clin. Breast Cancer.* 8 (2008) 392.
- [39] S. Diermeier, G. Horváth, R. Knuechel-Clarke, F. Hofstaedter, J. Szöllosi, G. Brockhoff, *Exp. Cell. Res.* 304 (2005) 604.

- [40] H. Huizhong. HER receptor-mediated dynamic signalling in breast cancer cells. PhD thesis. School of Molecular and Clinical Medicine, University of Edinburgh, Edinburgh, 2011.
- [41] A.C. Schmid, R.D. Byrne, R. Vilar, R. Woscholski, *FEBS Lett.* 566 (2004) 35.
- [42] J. Baselga, K.A. Gelmon, S. Verma, A. Wardley, P. Conte, D. Miles, G. Bianchi, J. Cortes, V.A. McNally, G.A. Ross, P. Fumoleau, L. Gianni, *J. Clin. Oncol.* 28 (2010) 1138.
- [43] H. Nakajima, K. Sakaguchi, I. Fujiwara, M. Mizuta, M. Tsuruga, J. Magae, N. Mizuta, *Biochem. Biophys. Res. Commun.* 356 (2007) 260.
- [44] S. Deleu, K. Choi, X. Pesesse, J. Cho, M.L. Sulis, R. Parsons, S.B. Shears, *Cell. Signal.* 18 (2006) 488.
- [45] J.T. Barata, *Adv. Enzyme Regul.* 51 (2011) 37.
- [46] J. Luo, *Cancer Lett.* 273 (2009) 194.
- [47] R.J. Orton, M.E. Adriaens, A. Gormand, O.E. Sturm, W. Kolch, D.R. Gilbert, *BMC Syst. Biol.* 3 (2009) 100.
- [48] B. Vanhaesebroeck, D.R. Alessi, *Biochem J.* 346 (2000) 561.
- [49] C. Peifer, D.R. Alessi, *ChemMedChem.* 3 (2008) 1810.
- [50] S. Deleu, K. Choi, X. Pesesse, J. Cho, M.L. Sulis, R. Parsons, S.B. Shears, *Cell. Signal.* 18 (2006) 488.
- [51] M.N. Bijman, M.P. van Berkel, M. Kok, M.L. Janmaat, E. Boven, *Anticancer Drugs* 20 (2009) 450.

## Figure legends

Fig. 1. Scheme of MAPK and PI3K/PTEN/AKT signalling network. Frames mark the influence regions of mutations or aberrant expression of the enzymes: frame 1 marks the influence region of *PIK3CA* mutation; frame 2 - PTEN loss; and frame 3 - GSK3 $\beta$  overexpression in the absence and presence (frames 1a, 2a, 3a, respectively) of HER2 inhibitor, pertuzumab (2C4).

Fig. 2. Dose response and sensitivity properties of the PI3K/PTEN/AKT signalling network. (A) pHER2 dose dependence for heregulin- $\beta$  (HRG) concentration (solid line), pAKT dose dependence for HRG in the absence (dashed line) and presence of PTEN inhibitor, 50 nM bpV(pic) (dotted line). (B) pHER2 and pAKT dose dependencies for pertuzumab (solid and dashed lines, respectively) at 95 nM and 1  $\mu$ M of HER2 concentration (thick and thin lines, respectively). Dotted line – pAKT dose dependence at three-fold increase in activity of CK2/GSK3 $\beta$  reaction of PTEN phosphorylation. Points on thick lines – experimental data (see Fig. 3 in [33]). (C) pHER2 and pAKT dose dependencies for HER2 concentration in the absence (thick solid and dashed lines, respectively) and presence of 100 nM pertuzumab (thin solid and dashed lines, respectively). (D) The dependence of sensitivities of the whole signalling network,  $S_{SN}$  (solid line), receptor subsystem  $S_{RSS}$  (dotted line), and signalling transaction subsystem  $S_{STS}$  (dashed line) on pertuzumab concentration. (E) Western blot analysis of the dose dependence of pHER2 (left) and pAKT (right) to HRG concentration (0 nM (control), 0.01 nM, 0.1 nM, 1 nM and 10 nM) at 5 and 30 minutes.

Fig. 3. The sensitivity of the signaling receptor system,  $S_{RSS,i}$  to (A) initial concentrations of HER2, HER3 receptors and HRG and (B) kinetic parameters of the HER2/HER3 receptor. Sensitivity values are derived from the model as calibrated using existing experimental data on pHER2 kinetics in the absence and presence of 100 nM pertuzumab (see Fig. 2A in [33]). The black and white bars correspond to  $S_{RSS,i}$  in the absence and presence of 100 nM pertuzumab, and grey bars - HER2 overexpression in the presence of 100 nM pertuzumab. Only sensitivities higher than 0.01 are shown.

Fig. 4. Input-output response and sensitivity characteristics of the signal transduction system, STS. (A) Dependence of pAKT output signal on pHER2 input signal of STS at different values of control parameter  $\gamma$ : solid line –  $\gamma=1$  (sensitive mode), dashed line –  $\gamma=0.5$

(resistance mode), dotted line –  $\gamma > 1$  (suppression mode). Arrows show the pAKT changes at the different perturbations of STS: arrow 1-2 corresponds to HER2 inhibition by 100 nM pertuzumab; 2-3 –  $\gamma$  decrease due to PTEN loss; 1-2\* –  $\gamma$  increase at PI3K inhibition by 1  $\mu$ M LY294002 combined with 100 nM pertuzumab. Points 2 and 3 – experimental data [32, 33]. (B) Sensitivity of STS to input signal, pHER2 for different  $\gamma$ . Line notations are as in Fig. 4A. The concentrations of pHER2 and pAKT are normalized to their maximal concentrations.

Fig. 5. Effects of HER2 inhibition and PTEN loss on sensitivity  $S_{STS,i}$  to the kinetic parameters of the enzymes involved in: (A) PI3K/PTEN cycle; (B) AKT phosphorylation; (C) sensitivity  $S_{STS,i}$  to initial concentrations of the enzymes and PIP2; and (D) sensitivity  $S_{STS,i}$  in the presence of PI3K inhibitor. Black bars – no pertuzumab, white bars – 100 nM pertuzumab, grey bars - 100 nM pertuzumab and PTEN inhibition by bpV(pic). Only sensitivities higher than 0.01 are shown. Comparison of the total sensitivity  $S$  (dark grey bars) with experimental data (see Fig. 4 in [33]) on pAKT inhibition by pertuzumab (light grey bars) for different inhibitor actions (E). Sensitivity  $S$  is normalised to maximal sensitivity in this series.

Fig. 6. (A) Western blot analysis of the inhibition effect on pAKT of varying concentrations of PTEN inhibitor, bpV(pic) (5 nM, 10 nM, 25 nM, 50 nM, 100 nM) at 1 nM heregulin, HRG in PE04 cells. (B) Theoretical pAKT dose dependence on PTEN concentration at saturated HRG signal (solid line) and at HER2 inhibition by pertuzumab (dashed line). Squares – experimental data on the dependence of pAKT concentration on PTEN expression level in 13 ovarian cancer lines (in relative units). Circles – experimental data on the dependence of pAKT concentration on PTEN expression for basal-like breast carcinoma (in relative units) [28]. (C) Experimental data (mean  $\pm$  S.D.,  $n=3$ ) on the effects of combinations of PDK1 inhibition by 7.5  $\mu$ M UCN-01, HER2 inhibition by 100 nM pertuzumab (2C4) and PTEN inhibition by 50  $\mu$ M bpV(pic).

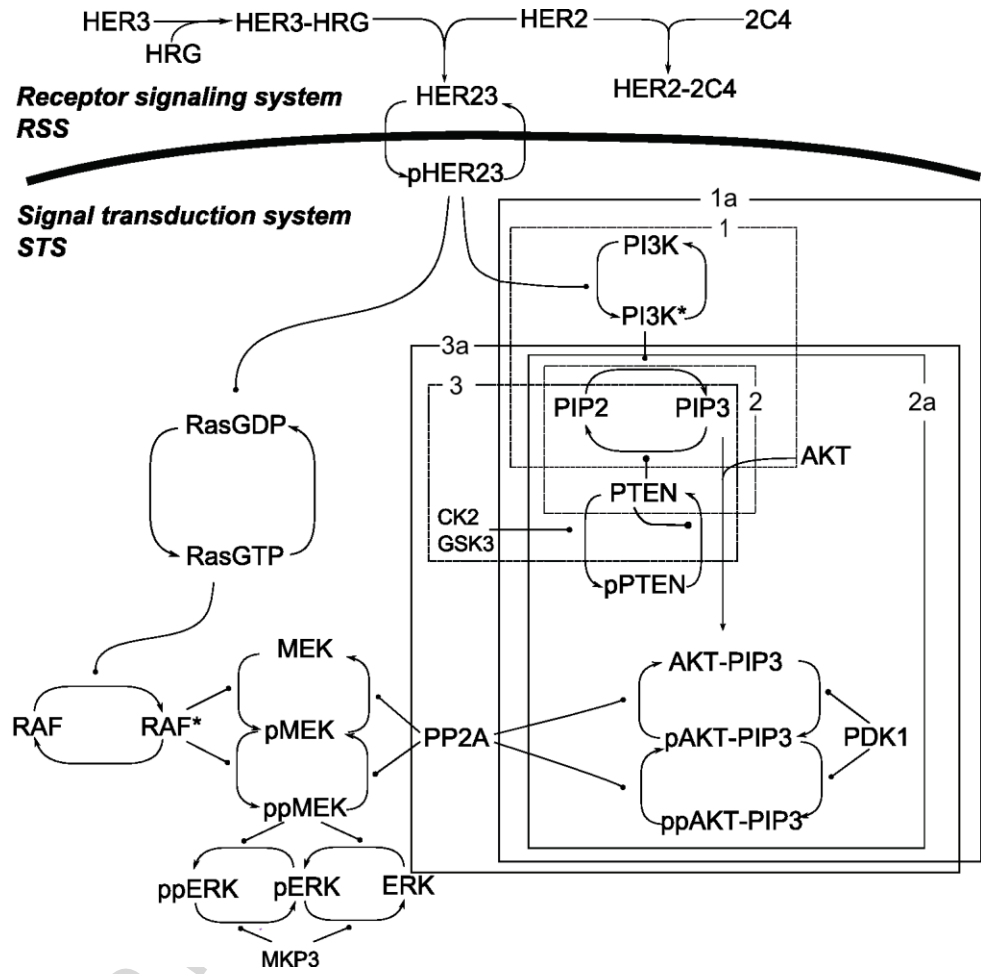


Fig. 1

ACCEPTED

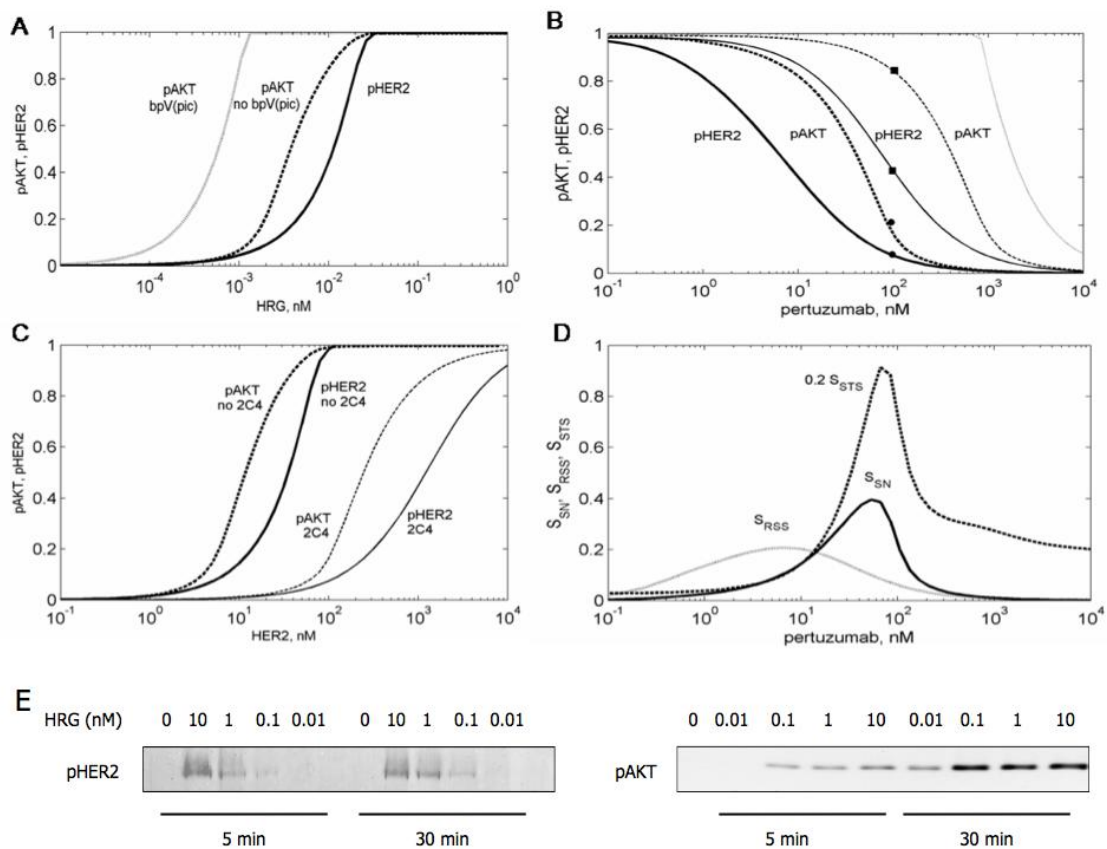


Fig. 2

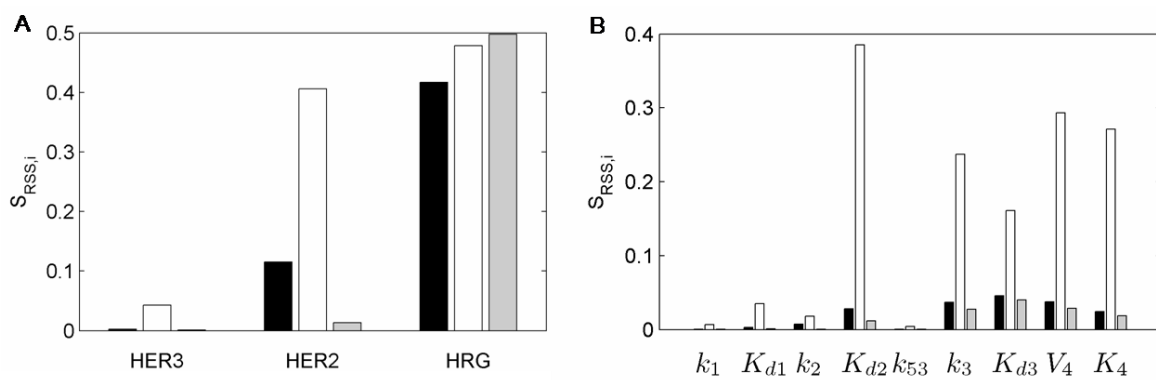


Fig. 3

ACCEPTED MANUSCRIPT

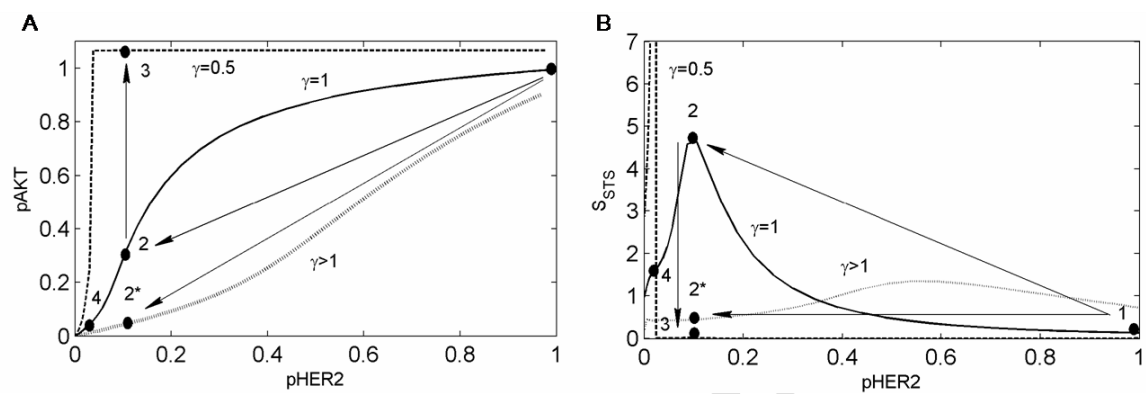


Fig. 4

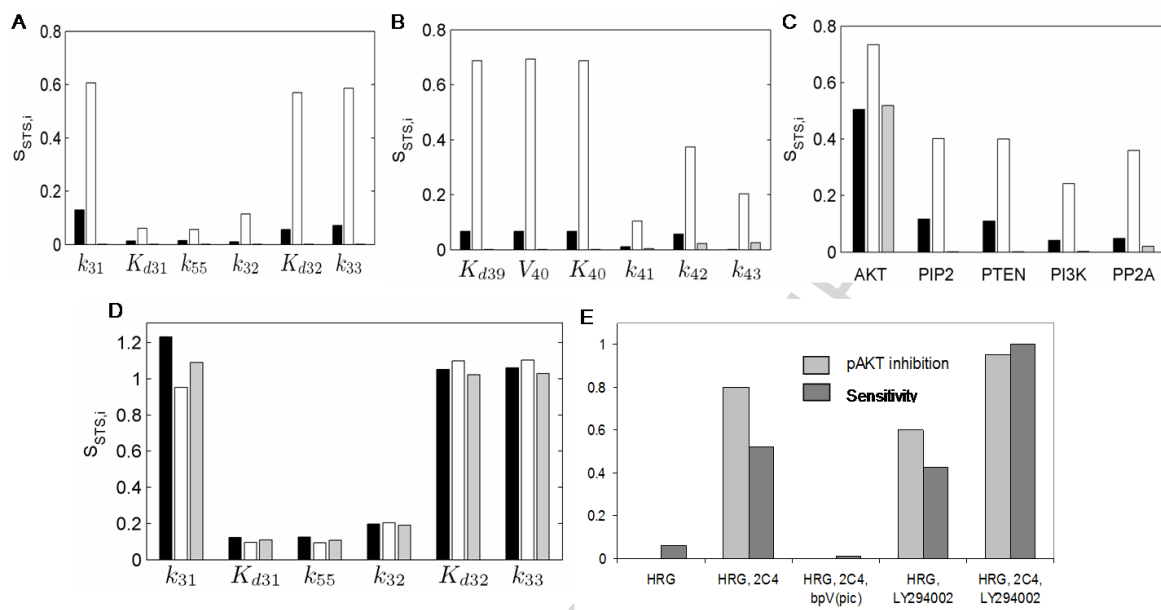


Fig. 5

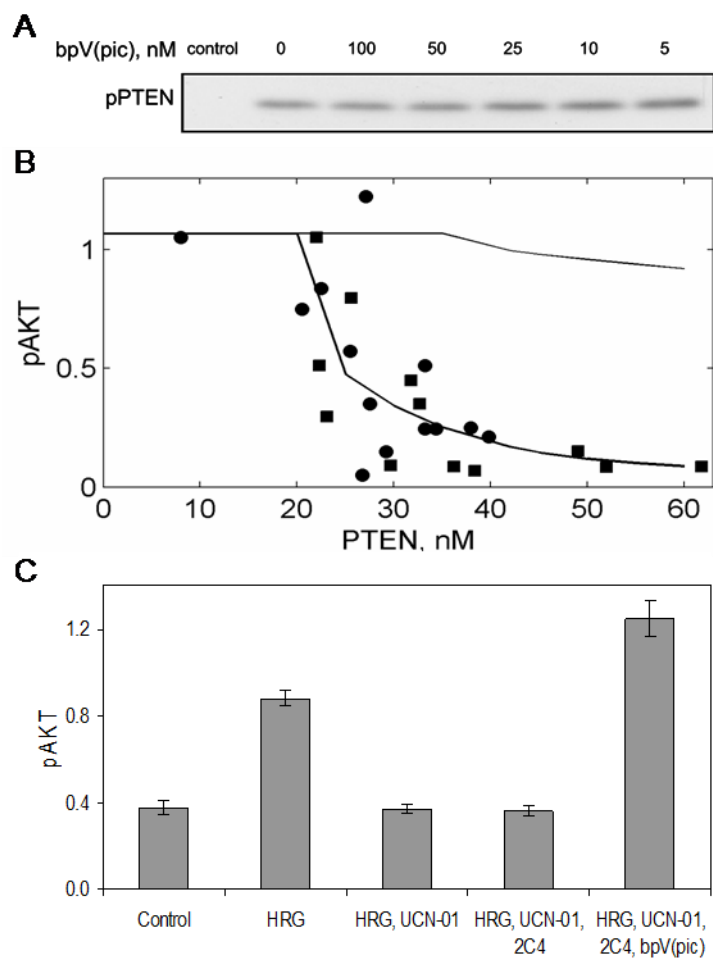


Fig. 6

## Highlights

- > We study the PI3K/PTEN/AKT signalling network and analyse network sensitivity
- > We model typical aberrations in this network identified in cancer and drug resistance
- > We find HER2 inhibition by pertuzumab increases signalling network sensitivity
- > PTEN loss or PI3CA mutation decreases network sensitivity
- > upstream inhibition abrogates pertuzumab resistance more effectively than downstream

ACCEPTED MANUSCRIPT